Humeral Epiphyseal Shape in the Felidae: The Influence of Phylogeny, Allometry and Locomotion

Anthony Walmsley,[1] Sarah Elton,[2] Julien Louys,[3-4] Laura C. Bishop, [3] and Carlo Meloro[2]

[1]Hull York Medical School, The University of York, Heslington York YO10 5DD, UK

[2]Hull York Medical School, The University of Hull, Loxley Building Cottingham Road, Hull HU6 7RX, UK

[3] Research Centre in Evolutionary Anthropology and Palaeoecology, School of Natural Sciences and Psychology, Liverpool John Moores University, Byrom Street, Liverpool L3 3AF, UK

[4] Present address: School of Earth Sciences, The University of Queensland, Brisbane, Australia

Running Header:

FELID HUMERAL MORPHOLOGY

Correspondence: Carlo Meloro, Hull York Medical School, The University of Hull, Loxley Building, Cottingham Road, Hull HU6 7RX, UK; T: ++44 (0)1904 321918; F: ++44 (0)1482 466497; carlo.meloro@hyms.ac.uk

ABSTRACT

Bone morphology of the cats (Mammalia: Felidae) is influenced by many factors, including locomotor mode, body size, hunting methods, prey size and phylogeny. Here, we investigate the shape of the proximal and distal humeral epiphyses in extant species of the felids, based on two-dimensional landmark configurations. Geometric morphometric techniques were used to describe shape differences in the context of phylogeny, allometry and locomotion. The influence of these factors on epiphyseal shape was assessed using Principal Component Analysis, Linear Discriminant functions and multivariate regression. Phylogenetic Generalised Least Squares was used to examine the association between size or locomotion and humeral epiphyseal shape, after taking a phylogenetic error term into account. Results show marked differences in epiphyseal shape between felid lineages, with a relatively large phylogenetic influence. Additionally, the adaptive influences of size and locomotion are demonstrated, and their influence is independent of phylogeny in most, but not all, cases. Several features of epiphyseal shape are common to the largest terrestrial felids, including a relative reduction in the surface area of the humeral head and increased robusticity of structures that provide attachment for joint-stabilising muscles, including the medial epicondyle and the greater and lesser tubercles. This increased robusticity is a functional response to the increased loading forces placed on the joints due to large body mass.

KEY WORDS**:** Felidae; humerus; geometric morphometrics; phylogeny; allometry; locomotion

INTRODUCTION

Accounting for more than ten percent of extant mammalian Carnivora, the Felidae are one of the most well-known families with well over 30 species found on all continents apart from Antarctica and Australia where no endemic species are recorded (Kitchener, 1991; Turner & Antón, 1997; Johnson et al., 2006; MacDonald et al., 2010). All felids are hypercarnivorous, specialised consumers of vertebrates (Kitchener, 1991; Turner & Antón, 1997; Kitchener et al., 2010). This common behaviour has generated relatively conservative cranial and mandibular morphology in the family when compared to other carnivorans (Holliday & Steppan, 2004; Meloro et al., 2008, 2011; Werdelin & Wesley-Hunt, 2010; Meloro, 2011a, b; Meloro & O'Higgins, 2011). In the felid postcranial skeleton, interspecific differentiation has been observed, in part because of adaptations to locomotion and posture (Gonyea, 1976; Van Valkenburgh, 1987; Anyonge, 1996; Andersson & Werdelin, 2003; Meachen-Samuels & Van Valkenburgh, 2009a), but also to adaptations for procuring prey of different sizes (Meachen-Samuels & Van Valkenburgh, 2009a, b, 2010; Lencastre Sicuro, 2011; Lencaster Sicuro & Oliveira, 2011; Meachen-Samuels, 2012) and due to specialisations for different modes of hunting (Christiansen, 2008; Slater & Van Valkenburgh, 2008). Notwithstanding these studies, there is still much to be explored regarding morphological variation in the felid postcranium and the factors, including phylogeny and allometry, that contribute to it.

Felid-like mammals originated in the Oligocene, around 35 million years ago. The earliest stem felid to be identified in the fossil record, *Proailurus*, was

recovered in the Quercy fissures (France) and is dated approximately 28.5 Ma. Molecular data suggest that the modern family Felidae arose within the last 11 million years (Johnson et al., 2006; Werdelin et al., 2010). Based on molecular evidence, the *Panthera* lineage (or clade), comprising the genera *Neofelis* (clouded leopard) and *Panthera* (lion, jaguar, leopard, tiger, snow leopard) is sister to all other extant members of the Felidae (Johnson et al., 2006). This clade originated around six million years ago, with considerable speciation in the genus *Panthera* occurring between around four and two million years ago (Johnson et al., 2006). Three other lineages, the Leopard Cat, Bay Cat and Caracal, diverged at the very end of the Miocene (5-6 Ma), with another, the Puma, originating just less than five million years ago (Johnson et al., 2006). The other lineages (Domestic Cat, Lynx, and Ocelot) diverged in the Pliocene, around three million years ago (Johnson et al., 2006).

Even with a common adaptation to hypercarnivory, the felids demonstrate a large range of body masses, a multitude of behaviours, and marked ecological diversity (Ewer, 1973; Turner & Antón, 1997; MacDonald et al., 2010). Members of the felid family range in size from under three kilograms (e.g. the black footed cat, *Felis nigripes*) to over 300 kilograms (the tiger, *Panthera tigris*). Felids exploit environments as diverse as open desert (e.g. the sand cat, *Felis margarita*), rainforest (e.g. the jaguar, *Panthera onca*), grassland (e.g. the lion, *Panthera leo*) and rocky, mountainous regions (e.g. the bobcat, *Lynx rufus*). Since locomotor mode correlates with the habitat exploited, felids show considerable diversity in locomotion, with some species engaging in

97 purely terrestrial locomotion and others demonstrating a high degree of
98 arboreality (Ewer, 1973; Kitchener, 1991; Kitchener et al., 2010).
99 Given the large size range within the felids, allometry is likely to play
100 some role in determining the shape of their postcranial skeletons (Mattern &
101 McLennan, 2000; Diniz-Filho & Nabout, 2009; Meachen-Samuels & Van
102 Valkenburgh, 2009a; Lewis & Lague, 2010). In addition, various studies have
103 implied that phylogeny influences bone morphology within both the carnivoran
104 cranium (Meloro et al., 2008, 2011; Meloro & O'Higgins, 2011) and postcranium
105 (Andersson & Werdelin, 2003; Meloro, 2011a). A small number of studies have
106 examined the relative importance of several factors determining postcranial
107 skeletal form in mammals (Monteiro & Abe, 1999; Young, 2008; Astúa,
108 2009),but most have focused on single contributory factors, such as locomotor
109 behaviour (Clevedon Brown & Yalden, 1973; Van Valkenburgh, 1987; Carrano,
110 1999; Schutz & Guralnick, 2007; Polly & MacLeod, 2008; Meloro, 2011c) or
111 allometry (Bertram & Biewener, 1990; Christiansen, 1999, 2002).
112 In this paper, we examine three factors - phylogeny, size and locomotion
113 – that, alongside other behaviours such as prey capture and foraging, are highly
114 likely to contribute to postcranial bone shape in the felids (Ewer, 1973; Van
115 Valkenburgh, 1987; Turner & Antón, 1997; Meachen-Samuels & Van
116 Valkenburgh, 2009a, 2010; Kitchener et al., 2010; Meachen-Samuels, 2012).
117 Our aim is to provide a detailed description of postcranial bone shape by
118 employing geometric morphometrics in order to quantitatively assess the impact
119 of these factors expressed as percentages of explained variance in shape (cf.
120 Caumul & Polly, 2005). Understanding the factors influencing shape is

important for successfully interpreting the evolutionary history and ecology of this diverse family, and provides a quantitative framework for analysing fossil species.

We focus on the humeral epiphyses partly because the humerus is argued to reflect function, in both felids (Meachen-Samuels & Van Valkenburgh, 2009a, 2010; Lewis & Lague, 2010) and other mammals, including primates and rodents (Elton, 2001, 2002, 2006; Samuels & Van Valkenburgh, 2008). As in primates, the shoulder of many felids is highly mobile and can be used to negotiate complex terrestrial and arboreal environments. Thus, the humerus is often a much better indicator of subtle locomotor differences than hindlimb bones, which tend to provide propulsion (Clevedon Brown & Yalden, 1973). Since the forelimb is load bearing (Day & Jayne, 2007; Doube et al., 2009), the humerus bone itself is also likely to be moulded by allometry, and one would expect the largest felids to exhibit the most robust humeri (Doube et al., 2009; Lewis & Lague, 2010). We thus have three specific research questions:

1. To what extent, if any, phylogeny explains shape variance in the felid humeral epiphyses.
2. To what extent, if any, allometric scaling influences the shape of the epiphyses.
3. To what extent, if any, function (specifically that related to locomotion) influences the shape of the epiphyses.

MATERIALS AND METHODS

Specimens and data collection

Our sample comprised 110 humeri of 32 extant felid species, obtained from collections held at the Natural History Museum London, the National Museum of Scotland and the Royal Museum for Central Africa, with data collected between June 2008 and July 2009 by Meloro. For each species we included the following number of specimens (in parentheses): *Acinonyx jubatus* (5), *Caracal caracal* (2), *Caracal aurata* (2), *Caracal serval* (6), *Felis chaus* (2), *Felis silvestris lybica* (3), *Felis margarita* (2), *Felis nigripes* (2), *Felis silvestris grampia* (9), *Lynx canadensis* (4), *Lynx lynx* (3), *Leopardus pardalis* (4), *Lynx pardinus* (2), *Lynx rufus* (1), *Leopardus wiedii* (1), *Leopardus geoffroy* (2), *Leopardus guigna* (1), *Neofelis nebulosa* (3), *Pardofelis badia* (1), *Pardofelis marmorata* (1), *Pardofelis temminckii* (1), *Prionailurus bengalensis* (4), *Puma concolor* (2), *Puma jagouaroundi* (1), *Panthera leo* (17), *Panthera onca* (3), *Panthera pardus* (12), *Panthera tigris* (4), *Panthera uncia* (4), *Prionailurus planiceps* (1), *Prionailurus rubiginosus* (1), *Prionailurus viverrinus* (4). Details about the studied material are listed for each individual skeletal element in Supplementary online material Table 1.

Two-dimensional images of the humeral epiphyses were captured using a Nikon d40 digital camera with a 200mm lens following a standard protocol. Specimens were placed at a minimum focal distance of one metre from the camera attached to a Manfrotto tripod. A spirit level was used to ensure that the top of the camera remained perpendicular to the specimen being photographed. Eighty two of the 110 images were of the left humerus; the remaining images, of right humeri, were flipped horizontally in tpsDig (version 2.12, Rohlf, 2008) prior to landmarking and analysis. The proximal epiphysis was photographed from

169 medial and lateral aspects, and the distal epiphysis from anterior and posterior
170 aspects. Data for the distal epiphysis were obtained for all 110 specimens,
171 whereas proximal data were obtained for only 109 specimens.

172 Landmarks describing the shape of each epiphysis were digitised by
173 Walmsley in tpsDig (Rohlf, 2008) (Fig. 1). Given the potential for increasing
174 statistical error when using Procrustes methods with relatively small sample
175 sizes (Rohlf, 2000, 2003a; Cardini & Elton, 2007), accuracy and precision of
176 landmarking and consequently the amount of digitisation error were assessed.
177 To do this, four specimens, chosen to represent the range of body masses of
178 species in the study, were selected for further landmarking. Two of these,
179 *Leopardus geoffroyi* and *Pardofelis temminckii*, represented species lying within
180 modal frequencies, another belonged to the species with the largest body mass,
181 *Panthera leo*, and the fourth to the species with the smallest body mass,
182 *Prionailurus rubiginosus*. Over a period of three days, each specimen was
183 landmarked according to the scheme illustrated in Fig. 1. Landmarking was
184 repeated a further three times during this period, producing a total of four
185 configurations per specimen. By calculating linear distances between landmarks
186 and assessing how these distances changed after each successive
187 landmarking, it was determined that error due to digitisation was minimal and
188 that landmarks could be repeated with confidence (Supplementary online
189 material Table 2).
190
191 **Data analysis – Geometric morphometrics (GMM)**

192 The software *morphologika* (O'Higgins & Jones, 2006) was used to
193 conduct Generalised Procrustes Analyses (GPA) and Principal Component
194 Analyses (PCA). GPA superimposes the raw coordinates of each landmark
195 configuration by removing the effects of translation and rotation, and also scales
196 these configurations by calculating a unit centroid size (defined as 'the square
197 root of the sum of squared Euclidean distances from each landmark to the
198 centroid of the landmarks') for each specimen (Bookstein, 1989; Adams et al.,
199 2004; Zelditch et al., 2004). After GPA the landmark configurations provided by
200 each specimen lie within the non-Euclidean, Kendall shape space. Specimens
201 are distributed about the mean landmark configuration and are spread
202 throughout this space according to differences in shape (Zelditch et al., 2004;
203 Chen et al., 2005). To analyse shape differences further, the spread of data
204 within the non-Euclidean space is projected onto a Euclidean, linear tangent
205 space (Rohlf, 1996). Interpretation of the resulting shape data requires PCA.
206 This method of analysis provides orthogonal axes (Principal Components, PCs)
207 that successively describe the major aspects of variance of the sample. With
208 the use of mean coordinates plus eigenvectors, PCA allows shape variance for
209 each PC to be demonstrated graphically (Zelditch et al., 2004; Chen et al.,
210 2005). In the present sample, analyses conducted using tpsSmall version 1.20
211 (Rohlf, 2003b) indicated there was a very strong correlation ($r = 0.999$) between
212 non-Euclidean and Euclidean tangent space. Thus, the linear tangent space
213 demonstrated by the PC plots reliably describes shape variance amongst
214 specimens.
215

Phylogeny

Specimens were grouped according to lineage (Johnson et al., 2006, Supplementary online material Table 1) in order to assess the extent of phylogenetic influence on shape. For each epiphyseal aspect, plots of PC1 vs. PC2 were produced. The shape variance demonstrated by the PC plots was visualised via transformation grids. These transformation grids, formed using thin plate splines, show the relative deformation of structures (Bookstein, 1991), in this case across each PC. The relationship between phylogenetic lineage and shape was investigated by creating dummy variables for each lineage, which were regressed against the multivariate shape data (all PCs). This determined the correlation between phylogeny and shape using a test equivalent to a MANOVA (multivariate analysis of variance), with significance calculated via the Wilks' Lambda test. This test, performed for each aspect of the whole sample (N=109 or 110) in tpsRegr version 1.37 (Rohlf, 2009), also indicates the percentage of shape variance explained by phylogeny.

Allometry

The influence of allometry on shape variance was investigated via multivariate regression (Monteiro, 1999) performed in *morphologika* (O'Higgins & Jones, 2006). Natural log (NLog) transformed centroid size values were regressed against all PCs collectively, with significance computed using the Wilks' Lambda. Transformation grids were used to illustrate changes in shape from the median sized specimens to the smallest and largest (based on NLog centroid size values).

240

241 **Locomotion**

242 Similar methods to those employed in the phylogeny multivariate
243 regression were used to examine the relationship between locomotor mode and
244 shape. Species were assigned to one of three locomotor categories,
245 'Terrestrial', 'Terrestrial but Climbs' and 'Terrestrial and Arboreal'
246 (Supplementary online material Table 1), based on classifications in Ortolani &
247 Caro (1996). Dummy variables for the three locomotor groups were regressed
248 against shape. Additionally, discriminant function analysis (DFA) was used to
249 explore the changes in shape, as well as size, across locomotor categories.
250 Both shape (PCs) and size (NLog centroid size) variables were used in
251 discriminant analyses, performed for each epiphyseal aspect in PASW version
252 18 (SPSS Inc., 2009) using a stepwise method (variables are entered into the
253 model if the significance level of their F value is less than 0.05, and they are
254 removed if the significance level is greater than 0.01) to select the variables
255 which best discriminate locomotor categories. Following a recent study (Meloro,
256 2011a), size has been included alongside shape variables (cf. Schultz &
257 Guralnick, 2007) to increase prediction likelihood of ecological categories. The
258 locomotor categories assigned *a priori* were the same as those used in the
259 regression analyses. Shape variance across each function was visualised by
260 regressing discriminant function scores against shape variables in tpsRegr
261 version 1.37 (Rohlf, 2009), with transformation grids at either extreme of the
262 axes demonstrating deformation from the mean shape. The locomotor groups of
263 the unclassified/unknown specimens were predicted based on data provided by

the discriminant functions. A 'leave-one-out' procedure was conducted as a cross validation.

Sensitivity analyses

In order to validate the efficacy of our discriminant models, to make predictions irrespective of unequal taxonomic sample size (Kovarovic et al., 2011), we performed two kinds of sensitivity analyses. First, we repeated the most accurate DFA after removing from the original sample all the specimens belonging to a particularly abundant taxon. We repeated the DFA by excluding first *Panthera leo* (N = 17, the most abundant 'Terrestrial' felid), then *Felis silvestris grampia* (N = 9, the most abundant 'Terrestrial but Climbs'), and finally *Neofelis nebulosa* (N = 3, representative of 'Terrestrial and Arboreal').

A second sensitivity analysis was conducted to test for the effect of sample size (number of specimens) or body mass (in grams, log transformed) on percentage of correctly classified specimens for the 32 extant species sampled. Non-parametric Spearman correlation was applied to identify positive or negative significant correlations based on the results from all the DFA models.

Phylogenetic Generalised Least Squares (PGLS)

PGLS regressions were performed for each epiphyseal aspect, to assess if differences in shape between specimens as described by locomotion or allometry alone were independent of phylogeny (or specifically whether they were independent of the lineage to which they belong). This method, which can

also be used for multivariate datasets, incorporates phylogeny as an error term within the regression models of shape variables on locomotion (transformed into dummy variables) or size (Martins & Hansen, 1997; Rohlf, 2001, 2006a; Adams, 2008). For these analyses, we computed the mean shape coordinates for each species, performing separate GPAs for each species subsample (cf. Meloro et al., 2008). Size for each species was represented by NLog centroid size averaged from multiple specimens. The phylogenetic covariance matrix was computed based on the topology and time of divergence (from Johnson et al., 2006) and then added as error term in the multivariate regression models in NTSYS 2.21c (Rohlf, 2006b).

RESULTS

Phylogeny

MANOVA indicates that shape differs significantly between lineages (Table 1). Phylogeny accounts for the greatest shape variance for the anterior aspect of the distal epiphysis and least for the medial aspect of the proximal epiphysis. For the lateral aspect of the proximal epiphysis, PC1 and PC2 collectively describe 88.09% of the shape variance (PC1, 58.93%; PC2, 29.16%) (Fig. 2A). Even though some overlap between lineages is evident, the Puma lineage tends to cluster at more negative PC1 values, whereas Ocelot, Leopard Cat and Domestic Cat lineages have more positive values. Specimens having extreme negative scores on PC1 have a greater tubercle that projects superiorly above the humeral head, and a humeral head with little posterior projection, whilst specimens with positive scores have a more superiorly and

312 posteriorly projecting humeral head with a wider articular surface. Lineages
313 overlap more on PC2, which describes the antero-posterior expansion of the
314 greater tubercle associated with reduction of the articulating area of the
315 humerus head (Fig. 2A).

316 For the medial aspect of the proximal epiphysis, PC1 and PC2 explain
317 69.07% of the shape variance (PC1, 35.99%; PC2, 33.08%). Overlap occurs
318 between lineages on both axes (Fig. 2B). However, specimens belonging to the
319 *Panthera* and Domestic Cat lineages exhibit negative PC1 and PC2 scores
320 respectively (Fig. 2B). PC1 describes variation in the posterior projection of the
321 humeral head associated with variation in the width of the lesser tubercle. On
322 PC2, specimens with the most negative scores have a more posteriorly
323 projecting humeral head and a greater tubercle with relatively little projection in
324 the superior plane.

325 For the anterior aspect of the distal epiphysis, PC1 and PC2 collectively
326 describe 72.94% of the shape variance (PC1, 62.69%; PC2, 10.25%). All
327 lineages tend to cluster well along PC1, although Ocelot specimens cluster
328 better on PC2 (Fig. 2C). On PC1, specimens at the positive end of the axis
329 have a more proximally positioned supracondyloid foramen and a relatively
330 smaller combined medio-lateral width of the trochlea and capitulum. On PC2,
331 from negative to positive, there is a relative superior-inferior expansion of the
332 trochlea and capitulum (Fig. 2C).

333 For the posterior aspect of the distal epiphysis, PC1 and PC2 collectively
334 describe 56.72% of the shape variance (PC1, 36.40%; PC2, 20.32%). Some
335 lineage-based clustering is evident (Fig. 2D), with *Panthera* specimens, for

example, being at the more positive end of PC1, with a relatively larger olecranon fossa area and relatively smaller trochlea/capitulum in the superior-inferior dimension. From negative to positive PC2 scores there is a relative reduction in the medial projection of the medial epicondyle and a decrease in the width of the distal portion of the trochlea and capitulum plus an expansion in olecranon fossa area.

Allometry

In multivariate regression, NLog centroid size was significantly correlated with shape for both aspects of each epiphysis (Table 2). Allometry explains more shape variance in the anterior aspect of the distal epiphysis than in the posterior aspect, and more in the lateral aspect of the proximal epiphysis compared to the medial. Shape changes in relation to changes in NLog centroid size values are illustrated in Fig. 3. On the lateral aspect of the proximal epiphysis, as NLog centroid size increases, there is a decrease in the humeral head surface area and a slight increase in the proximal projection of the greater tubercle (Fig. 3A). Inspection of transformation grids for the medial aspect of the proximal epiphysis (Fig. 3B) indicates that larger specimens have a relatively larger lesser tubercle. On the anterior aspect of the distal humerus (Fig. 3C), larger specimens have a relatively larger combined width of trochlea and capitulum with a shorter and broader medial epicondyle. Differences on the posterior aspect of the distal epiphysis are less marked, although specimens with high NLog centroid size values show an increase in the olecranon fossa area (Fig. 3D).

360

361 **Locomotion**

362 MANOVA indicates that shape differs significantly between locomotor
363 categories for both proximal and distal epiphyses although, in general,
364 locomotor differences account for much less shape variance than do either
365 phylogeny or allometry (Table 3). In DFA, two significant functions were
366 extracted for each aspect except the posterior distal epiphysis (Table 4). Table
367 5 lists the variables selected after the stepwise for the DFA models, with NLog
368 centroid size being included in three of the four models. Reclassification rates
369 using the 'leave one out' method (Table 6) were above chance for each aspect
370 of the epiphyses, with the anterior aspect of the distal epiphysis being the
371 region that best discriminated between different locomotor groups.

372 The DFA plots show some discrimination between locomotor groups
373 even if overlap occurs among specimens (Fig. 4). Terrestrial specimens tend to
374 occupy positive scores of DF1 in all structures except in the anterior aspect of
375 the distal epiphysis (Fig. 4C). For the proximal epiphysis positive scores of DF1
376 are associated to short articular surface and a wide lesser tubercle (Figs. 4A,
377 B). 'Terrestrial and Arboreal' specimens tend to occupy positive scores of
378 Function 2 for the lateral aspect of the proximal epiphysis, characterised by less
379 superiorly projecting humeral head (Fig. 4A). However, they overlap
380 extensively with 'Terrestrial but Climbs' specimens and this is reflected in the re-
381 classification rate (Table 6).

382 For the distal epiphysis, terrestrial specimens have positive scores of
383 DF1 that describe a relatively wide medial epicondyle and a large medio-lateral

384 width of the trochlea (Fig. 4C). Interestingly, Terrestrial and Arboreal specimens
385 share a wider medial epicondyle with a larger superior-inferior dimension of the
386 trochlea and the supracondyloid foramen on the anterior aspect of the distal
387 epiphysis (Fig. 4C). The posterior aspect of the distal epiphysis does not
388 differentiate locomotor groups on either function (Fig. 4D).

389 As the medial aspect of the proximal epiphysis and the anterior aspect of
390 the distal epiphysis are the best predictors of locomotor category (Table 6), the
391 functions formed by their shape and size variables are used to predict the
392 locomotor categories for the four specimens of unclassified/unknown
393 locomotion. In the case of the medial aspect of the proximal epiphysis,
394 *Pardofelis badia* and *Pardofelis temminckii* are classified as 'Terrestrial and
395 Arboreal' and both *Felis nigripes* specimens are classified as 'Terrestrial but
396 Climbs'. For the anterior aspect of the distal epiphysis, *Pardofelis badia* and
397 both *Felis nigripes* specimens are classified as 'Terrestrial and Arboreal',
398 whereas *Pardofelis temminckii* is classified as 'Terrestrial but Climbs'.

399

400 **Sensitivity Analyses**

401 The percentage of correctly classified specimens differs between species
402 (Table 7). With regard to species with more than one representative specimen,
403 the lion (*Panthera leo*), the snow leopard (*Panthera uncia*) and the cheetah
404 (*Acinonyx jubatus*) appear to be the best classified in the analyses. There is a
405 significant association between body size and number of specimens per
406 species ($r = 0.62$, $p = 0.0003$), but no other factor, including lineage and sample
407 size, affects the reclassification rate.

Separately excluding *Panthera leo*, *Neofelis nebulosa* and *Felis silvestris* specimens (representing the species of largest sample size for each locomotor group) from the discriminant function analyses, does not have a major impact on the reclassification rate of the original DFA models (Table 8). In all cases, the repeated DFA models are statistically significant. There is a small degree of change however, with the exclusion of *Panthera leo* decreasing the reclassification rate for both aspects of proximal epiphyses, whilst removing the *Felis silvestris* sample improved models based on the lateral aspect of proximal epiphysis and the posterior aspect of distal epiphysis. The exclusion of the only three specimens of *Neofelis nebulosa* generally improved reclassification in all the models except for anterior aspect of the distal epiphysis (Table 8).

PGLS

The PGLS models (Table 9), which incorporate phylogeny as an error term, indicate that allometry has a significant independent influence on humeral epiphyseal shape, except for the anterior aspect of the distal epiphysis. Locomotion has a significant independent influence on the shape of the humeral epiphyses, with the exception of the medial aspect of the proximal epiphysis.

DISCUSSION

In common with previous research on the felid postcranium (Van Valkenburgh, 1987; Andersson & Werdelin, 2003; Andersson, 2004; Christiansen & Harris, 2005; Doube el al., 2009; Meachen-Samuels & Van Valkenburgh, 2009a), we find clear interspecific variation in long bone

morphology. Phylogeny, allometry and locomotion all influence humeral epiphyseal shape in our sample, with phylogeny and allometry contributing more than locomotion.

Phylogenetic signals in postcranial and cranial shape have been noted among Carnivora as a whole (Radinsky, 1981; Andersson & Werdelin, 2003; Andersson, 2004; Meloro et al., 2008, 2011; Meloro, 2011a, b, c; Meloro & O'Higgins, 2011; Slater & Van Valkenburgh, 2008). MANOVA and PCA in the present study indicate a marked phylogenetic signal in the shape of the humeral epiphyses within the Felidae. For the shape of each aspect of both epiphyses the *Panthera* lineage emerges as one of the most distinctive. This maybe a result of its early divergence from all other cat lineages (Johnson et al., 2006). Such distinctiveness has also been noted in ecomorphological analyses of felid skulls (Werdelin, 1983; Slater & Van Valkenburgh, 2008; Lencastre Sicuro, 2011; Lencastre Sicuro & Oliveira, 2011) and it is apparent when mapping averaged PC1 scores for all the four epiphyseal aspects onto the phylogenetic topology (Fig. 5).

In PCA, members of the *Panthera* lineage tend to form a coherent group separated from most other specimens. This is particularly striking given that the group comprises purely terrestrial, terrestrial with climbing and mixed terrestrial and arboreal species, with a large body mass range (some species being over 150 kg and others under 20kg). However, this diversity is evident in the PC plots and mapping (Figs. 2 and 5). Although the lineage clusters have relatively little overlap with other lineages, wide ranges of scores are still obtained for *Panthera* specimens, for both aspects of the proximal humerus and the

posterior aspect of the distal humerus. This reflects the biological and ecological diversity of modern members of the lineage, which speciated rapidly in the Pliocene (Johnson et al., 2006). Among the other felid lineages, there is considerable overlap on the plots of PC1 versus PC2. Members of the non-*Panthera* lineages tend to be relatively small (17 out of the 26 non-*Panthera* lineage species sampled are under 10kg), and that may account for some overlap, especially since lineages mostly comprising small species tend to be dominated by climbing or arboreal forms, which may create additional convergence. Based on PC1 character mapping, this occurs consistently in the 'Leopard Cat' and 'Domestic Cat' lineages that show a limited variation especially in the lateral aspect of proximal epiphysis and anterior aspect of the distal epiphysis (Fig. 5).

The influence of size on cranial and postcranial morphology has been noted within and between several families of the order Carnivora (Schutz & Guralnick, 2007; Meloro et al., 2008, 2011; Meachen-Samuels & Van Valkenburgh, 2009b; Meloro 2011b). In this study, allometry was a significant influence on humeral epiphyseal shape (accounting for 17–40% of variance), independent of phylogeny for all but the anterior aspect of the distal epiphysis. Allometry explained a reasonably large amount of shape variance for the lateral aspect of the proximal epiphysis. The largest specimens require the greatest amount of stability at the joint to account for increased loading forces. These demonstrate a reduced humeral head surface area, limiting the degree of movement at the shoulder joint, and a more superiorly projecting greater tubercle to reduce rotational movement and to provide a greater surface area

480 for insertion of the stabilising rotator cuff muscles (Kappelman, 1988; Turner &
481 Antón, 1997).
482 The shape of the anterior aspect of the distal epiphysis in larger specimens may
483 demonstrate adaptations for stability, including an increased projection of the
484 medial epicondyle for the attachment of muscles that allow pronation-supination
485 as well as flexing digits (i.e. M. pronator teres; M. palmaris longus; third and
486 fourth parts of M. flexor profundus digitorum; M. flexor carpi radialis; second
487 head of M. flexor profundus digitorum; page 171, Reighard & Jennings, 1901).
488 The elbow joint is load bearing, and it has been demonstrated that felid limbs
489 respond to increased body size, and therefore increased loading, via allometric
490 shape change (Doube et al., 2009), so larger species and specimens are more
491 robust. In felids the influence of allometry has been suggested to be much
492 stronger at the epiphyses than at the shaft, due to tension from muscle and
493 ligament attachments and due to shear and torsion from joint loading (Doube et
494 al., 2009). This allometric pattern is unique to felids, as other carnivoran families
495 (with species exhibiting body masses of less than 300 Kg), such as canids,
496 respond to an increase in body size by limb straightening (Day & Jayne, 2007;
497 Meachen-Samuels & Van Valkenburgh, 2009a).
498 Interestingly, PGLS shows that size influence is dependent on phylogeny
499 in the anterior aspect of distal epiphysis, suggesting that there is a very strong
500 phylogenetic signal in this region of the bone. The significant independent
501 contribution of locomotion in influencing the anterior distal humerus morphology
502 suggests that there has also been strong selective pressure on this region that
503 is not simply explained by size or conserved morphology. The assertion of

504 strong selective pressure for the anterior distal epiphysis is reinforced by the
505 reasonably high classification accuracy in discriminant analysis across all
506 locomotor groups (in general, better than the proximal epiphysis or posterior
507 distal aspect for all locomotor categories).

508 DFA and PGLS indicate that locomotion influences humeral epiphyseal
509 shape, further confirming the association between locomotion and mammalian
510 postcranial shape noted in previous studies (Van Valkenburgh, 1987;
511 Kappelman, 1988; Gebo & Rose, 1993; Plummer & Bishop, 1994; Elton, 2001,
512 2002; Schutz & Guralnick, 2007; Meachen-Samuels & Van Valkenburgh,
513 2009b; Meloro 2011a). This notwithstanding, locomotion explained the least
514 amount of humeral epiphyseal shape variance (between 5 and 16%) in our
515 sample. For the medial aspect of the proximal epiphysis, for which locomotion
516 explained the least variance (5%), PGLS indicated that this influence was
517 dependent on phylogeny.

518 The mean reclassification rate for the whole DFA was 65%, relatively
519 modest compared to studies of other mammals (Kappelman, 1988; Plummer &
520 Bishop, 1994; Bishop, 1999; Elton, 2001), but similar to the rate observed in an
521 earlier study (Meachen-Samuels & Van Valkenburgh, 2009a) of felid forelimb
522 shape that used a different locomotor categorisation system that divided the
523 sample into terrestrial, arboreal and scansorial specimens. Based on data from
524 Ortolani & Caro (1996), the majority of cats are at least partially terrestrial,
525 which may have assisted their extensive dispersal and cosmopolitan range
526 (sensu Hughes et al., 2008). This widespread terrestriality across species

527 inevitably results in morphological similarity, either because of shared ancestry
528 or convergence, which in turn is reflected in the discriminant analysis.
529 The DFA classification accuracy rate for the anterior aspect of the distal
530 epiphysis was surprisingly high in the 'Terrestrial but Climbs' category, given the
531 range of species and body masses included and in marked contrast to the
532 modest classification rates of the other humeral aspects for this category. The
533 landmark set for the anterior aspect of the distal humerus captures two
534 important components of the elbow joint: the trochlea, which articulates with the
535 ulna and the capitulum which articulates with the radial head, as well as the
536 medial epicondyle, the origin for mm. flexor carpi radialis, mm. flexor carpi
537 ulnaris, mm. flexor digitorum superficialis (all flexors of the manus) and the
538 manual pronator mm. pronator teres (Kardong & Zalisko, 2002). It is possible
539 that the good separation between 'Terrestrial but Climbs' and other felid
540 specimens reflects differences in manual flexion and pronation in climbing cats.
541 Discrimination was poor for the posterior aspect of the distal epiphysis, a result
542 consistent with the multivariate regression. Given the results for the anterior
543 aspect of the distal humerus, this result may seem anomalous, as the anterior
544 and posterior aspects are part of the same structure. However, the dominant
545 feature of the posterior distal humerus, the olecranon fossa, has been shown in
546 previous studies, albeit in primates, to be highly morphologically variable (Elton,
547 2001).
548 For the proximal humerus, as well as the posterior distal epiphysis, large
549 scatters around centroids were evident, with extensive overlap between
550 categories. In our study, there was reasonably high general classification

accuracy in the ‘Terrestrial’ sample. This reflects, in part, adaptations for terrestriality (including a humeral head with a relatively decreased surface area, and an increased lesser tubercle width and greater tubercle projection for insertion of the rotator cuff muscles) which stabilise the limb and constrain movement mainly to the parasagittal plane, important when chasing prey in open environments (Kappelman, 1988; Gebo & Rose, 1993; Turner & Antón, 1997).

Additionally, our sensitivity analyses demonstrate that DFA models were always accurate irrespective of sample size and species selection. Classification rate varies across species but this variation has no pattern and is not systematically influenced by any ecological or phylogenetic factor. On the other hand, the exclusion of particular taxa from our sample confirms DFA model stability, where accuracy appears to be unchanged or even increased in some cases. This allows us to interpret with confidence the classification of unknown specimens. The classification of *Pardofelis badia* and *Pardofelis temminckii* is consistent with an arboreal lifestyle. This is likely to reflect the strong phylogenetic component observed in all humeral epiphyses, as these species appear to be classified within the same group as their sister species *Pardofelis marmorata* (Johnson et al., 2006). The same applies for *Felis nigripes*, a species that one would expect to be classified as a terrestrial species (cf. Meachen-Samuels & Van Valkenburgh, 2009), but is in fact classified as a either ‘Terrestrial but Climbs’ or ‘Terrestrial and Arboreal’. It is likely that this species retained ancestral adaptations for climbing in humeral

574 morphology that are not needed for its current habitat preference (short
575 grassland of Southern Africa, (MacDonald et al., 2010).
576 In summary, we have found that whilst the shape of humeral epiphyses
577 is strongly informative of Felidae evolutionary history, size and locomotion exert
578 an adaptive influence on their interspecific shape variation. Our study provides
579 a solid baseline to extend two dimensional geometric morphometric analyses to
580 other long bone epiphyses, as well as other mammals.
581

582 ## ACKNOWLEDGEMENTS

583 We would like to thank museum curators and staff at British Museum of
584 Natural History (NHM, London), the Royal Museum of Scotland (RMS,
585 Edinburgh) and the Royal Museum for Central Africa (RMCA, Tervuren) for
586 kindly providing access and support to the study of felid skeletal specimens. In
587 particular, we are grateful to: P. Jenkins, L. Tomsett, R. Portela-Miguez, A.
588 Salvador, and D. Hills (NHM); A. Kitchener and J. Herman (RMS); E. Gilissen
589 and W. Wendelen (RMCA). The data collection from the Royal Museum for
590 Central Africa was undertaken thanks to a SYNTHESYS grant to C. Meloro for
591 the project 'Ecomorphology of extant African carnivores' (BE-TAF 4901). Our
592 research was generously supported by the Leverhulme Trust project "Taxon-
593 Free Palaeontological Methods for Reconstructing Environmental Change"
594 (F/00 754/C). We thank the Editor, M. Starck, and two anonymous reviewers for
595 useful suggestions that improved the quality of this manuscript.
596

597 ## LITERATURE CITED

598 Adams DC, Rohlf FJ, Slice DE. 2004. Geometric morphometrics: ten years of
599 progress following the ‘revolution’. Ital J Zool 71:5–16.
600 Adams DC. 2008. Phylogenetic meta-analysis. Evolution 62:567–572.
601 Andersson KI, Werdelin L. 2003. The evolution of cursorial carnivores in the
602 Tertiary: implications of elbow-joint morphology. Proc Roy Soc Lond B (Suppl)
603 270:S163–S165.
604 Andersson KI. 2004. Elbow-joint morphology as a guide to forearm and foraging
605 behaviour in mammalian carnivores. Zool J Linn Soc 142:91–104.
606 Anyonge W. 1996. Locomotor behaviour in Plio-Pleistocene sabre-tooth cats: a
607 biomechanical analysis. J Zool 238:395–413.
608 Astúa D. 2009. Evolution of scapula size and shape in didelphid marsupials
609 (Didelphimorphia: Didelphidae). Evolution 63:2438–2456.
610 Bertram JEA, Biewener AA. 1990. Differential scaling of the long bones in the
611 terrestrial Carnivora and other mammals. J Morphol 204:157–169.
612 Bishop LC. 1999. Suid paleoecology and habitat preference at African Pliocene
613 and Pleistocene hominid localities. In: Bromage TG & Schrenk F, editors.
614 African Biogeography, Climate Change and Early Hominid Evolution. New York:
615 Oxford University Press. p 216–225.
616 Bookstein FL. 1989. Size and shape: a comment on semantics. Syst Zool
617 38:173–180.
618 Bookstein FL. 1991. Morphometric tools for landmark data. Geometry and
619 Biology. Cambridge: Cambridge University Press.
620 Cardini A, Elton S. 2007. Sample size and sampling error in geometric
621 morphometric studies of size and shape. Zoomorphology 126:121–134.

622 Carrano MT. 1999. What, if anything, is a cursor? Categories vs. continua for
623 determining locomotor habit in mammals and dinosaurs. J Zool 247:29–42.
624 Caumul R, Polly PD. 2005. Phylogenetic and environmental components of
625 morphological variation: skull, mandible, and molar shape in marmots
626 (Marmota, Rodentia). Evolution 57:2460–2472.
627 Chen X, Milne N, O' Higgins P. 2005. Morphological variation of the
628 thoracolumbar vertebrae in Macropodidae and its functional relevance. J
629 Morphol 266:167–181.
630 Christiansen P. 1999. Scaling of the limb long bones to bodymass in terrestrial
631 mammals. J Morphol 239:167–190.
632 Christiansen P. 2002. Mass allometry of the appendicular skeleton in terrestrial
633 mammals. J Morphol 251(2):195–209.
634 Christiansen P, Harris M. 2005. Body size of *Smilodon* (Mammalia: Felidae). J
635 Morphol 266:369–384.
636 Christiansen P. 2008. Evolution of skull and mandible shape in cats (Carnivora:
637 Felidae). PLoS ONE 3:e2807.
638 Clevedon Brown J, Yalden DW. 1973 The description of mammals-2 Limbs and
639 locomotion of terrestial mammals. Mammal Rev 3:107–134.
640 Day LM, Jayne BC. 2007. Interspecific scaling of the morphology and posture of
641 the limbs during the locomotion of cats (Felidae). J Exp Biol 210:642–654.
642 Diniz-Filho JAF, Nabout JC. 2009. Modeling body size evolution in Felidae
643 under alternative phylogenetic hypotheses. Genet Mol Biol 32:170–176.

644 Doube M, Wiktorowicz-Conroy A, Christiansen P, Hutchinson JR, Shefelbine S.
645 2009. Three-dimensional geometric analysis of felid limb bone allometry. PLoS
646 ONE 4:e4742.
647 Elton S. 2001. Locomotor and habitat classification of cercopithecoid postcranial
648 material from Sterkfontein Member4, Bolt's Farm and Swartkrans Members 1
649 and 2, South Africa. Palaeontologia africana 37:115–126.
650 Elton S. 2002. A reappraisal of the locomotion and habitat preference of
651 Theropithecus oswaldi. Folia Primatol 73:252–280.
652 Elton S. 2006. 40 years on and still going strong: the use of the hominin-
653 cercopithecid comparison in human evolution. J Roy Anthropol Inst 12:19–38.
654 Ewer RF. 1973. The carnivores. New York: Cornell University Press.
655 Gebo DL, Rose KD. 1993. Skeletal morphology and locomotor adaptation in
656 *Prolimnocyon atavus*. J Vertebr Paleont 13:125–144.
657 Gonyea WJ. 1976. Behavioural implications of saber-toothed felid morphology.
658 Paleobiology 2:332–342.
659 Holliday JA, Steppan SJ. 2004. Evolution of hypercarnivory: the effect of
660 specialization on morphological and taxonomic diversity. Paleobiology 30:108–
661 128.
662 Hughes JK, Elton S, & O'Regan HJ. 2008. Theropithecus and 'Out of Africa'
663 dispersals in the Plio-Pleistocene. J Hum Evol 54:43–77.
664 Johnson WE, Eizirik E, Pecon-Slattery J, Murphy WJ, Antunes A, Teeling E,
665 O'Brien SJ. 2006. The late Miocene radiation of modern Felidae: a genetic
666 assessment. Science 311:73–77.

667 Kappelman J. 1988. Morphology and locomotor adaptations of the bovid femur
668 in relation to habitat. J Morphol 198:19–130.
669 Kardong KV, Zalisko EJ. 2002. Comparative Vertebrate Anatomy: A Laboratory
670 Dissection Guide. Boston: McGraw-Hill.
671 Kitchener A. 1991. The Natural History of the Wild Cats. New York: Comstock
672 Publishing Associates.
673 Kitchener AC, Van Valkenburgh B, Yamaguchi N. 2010. Felid form and function.
674 In: MacDonald DW, Loveridge AJ, editors. Biology and Conservation of Wild
675 Felids. Oxford: Oxford University Press. p 83–106.
676 Kovarovic K, Aiello LC, Cardini A, Lockwood CA. 2011. Discriminant Function
677 Analysis in archaeology: are classification rates too good to be true? J Archaeol
678 Sci 38:3006–3018.
679 Lencastre Sicuro F. 2011. Evolutionary trends on extant cat skull morphology
680 (Carnivora: Felidae): a three-dimensional geometrical approach. Biol J Linn Soc
681 103:176–190.
682 Lencastre Sicuro F, Oliveira FB. 2011. Skull morphology and functionality of
683 extant Felidae (Mammalia: Carnivora): a phylogenetic and evolutionary
684 perspective. Zool J Linn Soc 161:414–462.
685 Lewis ME, Lague MR. 2010. Interpreting sabretooth cat (Carnivora; Felidae;
686 Machairodontinae) postcranial morphology in light of scaling patterns. In:
687 Goswami A, Friscia AR, editors. Carnivoran Evolution. New views on
688 phylogeny, form and function. Cambridge: Cambridge University Press. p 411–
689 465.

690 MacDonald DW, Loveridge AJ, Nowell K. 2010. *Dramatis personae*: an
691 introduction to the wild felids. In: MacDonald DW, Loveridge AJ, editors. Biology
692 and Conservation of Wild Felids. Oxford: Oxford University Press Oxford. p 3–
693 58.
694 Maddison DR, Maddison WP. 2000. MacClade version 4: Analysis of phylogeny
695 and character evolution. Sinauer Associates, Sunderland Massachusetts.
696 Martins EP, Hansen TF. 1997. Phylogenies and the comparative method: a
697 general approach to incorporating phylogenetic information into the analysis of
698 interspecific data. Am Nat 149:646–667.
699 Mattern MY, McLennan DA. 2000. Phylogeny and speciation of felids. Cladistics
700 16:232–253.
701 Meachen-Samuels J, Van Valkenburgh B. 2009a. Forelimb indicators of prey-
702 size preference in the Felidae. J Morphol 270:729–744.
703 Meachen-Samuels J, Van Valkenburgh B. 2009b. Craniodental indicators of
704 prey size preference in the Felidae. Biol J Linn Soc 96:784–799.
705 Meachen-Samuels J, Van Valkenburgh B. 2010. Radiographs reveal
706 exceptional forelimb strength in the sabertooth cat, Smilodon fatalis. PLoS ONE
707 5:e11412.
708 Meachen-Samuels J. 2012. Morphological convergence of the prey-killing
709 arsenal of sabertooth predators. Paleobiology 38:1–14.
710 Meloro C, Raia P, Piras P, Barbera C, O'Higgins P. 2008. The shape of the
711 mandibular corpus in large fissiped carnivores: allometry, function and
712 phylogeny. Zool J Linn Soc 154:832–845.

713 Meloro C. 2011a. Feeding habits of Plio-Pleistocene large carnivores as
714 revealed by their mandibular geometry. J Vertebr Paleont 31:428–446.
715 Meloro C. 2011b. Morphological disparity in Plio-Pleistocene large carnivore
716 guilds from Italian peninsula. Acta Palaeontol Pol 56:33–44.
717 Meloro C. 2011c. Locomotor adaptations in Plio-Pleistocene large carnivores
718 from the Italian peninsula: Palaeoecological implications. Current Zoology
719 57:269–283.
720 Meloro C, O' Higgins P. 2011. Ecological adaptations of mandibular form in
721 fissiped Carnivora. J Mamm Evol 18:185–200.
722 Meloro C, Raia P, Carotenuto F, Cobb S. 2011. Phylogenetic signal, function
723 and integration in the subunits of the carnivoran mandible. Evol Biol 38:465–
724 475.
725 Monteiro LR. 1999. Multivariate regression models and geometric
726 morphometrics: the search for causal factors in the analysis of shape. Syst Biol
727 48:192–199.
728 Monteiro LR, Abe AS. 1999. Functional and historical determinants of shape in
729 the scapula of Xenarthran mammals: evolution of a complex morphological
730 structure. J Morphol 241:251–263.
731 O' Higgins P, Jones N. 2006. Morphologika 2.5, York: Function morphology &
732 evolution research group, Hull York Medical School.
733 Ortolani A, Caro TM. 1996. The adaptive significance of color patterns in
734 carnivores: phylogenetic tests of classic hypotheses. In: Gittleman JL, editor.
735 Carnivore Behaviour, Ecology, and Evolution, Vol. 2. New York: Cornell
736 University Press. p 132–188.

737 Plummer TW, Bishop LC. 1994. Hominid Paleoecology at Olduvai Gorge,
738 Tanzania as indicated by antelope remains. J Hum Evol 27:47–75.
739 Polly PD, Macleod N. 2008. Locomotion in fossil carnivora: an application of
740 eigensurface analysis for morphometric comparison of 3D surfaces.
741 Palaeontologia Electronica 11.2.8A.
742 Radinsky LB. 1981. Evolution of skull shape in carnivores, 1: representative of
743 modern carnivores. Biol J Linn Soc 15:369–388.
744 Reighard JE, Jennings, HS. 1901. Anatomy of the Cat. New York: H. Holt.
745 Rohlf FJ. 1996. Morphometric spaces, shape components and the effect of
746 linear transformations. In: Marcus LF, Corti M, Loy A, et al., editors. Advances
747 in morphometrics. New York: Plenum Press. p 131–129.
748 Rohlf FJ. 2000. On the use of shape spaces to compare morphometric
749 methods. Hystrix Ital J Mamm 11:8–24.
750 Rohlf FJ. 2001. Comparative methods for the analysis of continuous variables:
751 geometric interpretations. Evolution 55:2143–2160.
752 Rohlf FJ. 2003a. Bias and error in estimates of mean shape in morphometrics. J
753 Hum Evol 44:665–683.
754 Rohlf FJ. 2003b. tpsSmall1.20. Stony Brook, NY: Department of Ecology and
755 Evolution, State University of New York.
756 Rohlf FJ. 2006a. A comment on phylogenetic correction. Evolution 60:1509–
757 1515.
758 Rohlf FJ. 2006b. NTSYSpc 2.21c. New York: Exeter Software.
759 Rohlf FJ. 2008. tpsDig2.12. Stony Brook, NY: Department of Ecology and
760 Evolution, State University of New York.

761 Rohlf FJ. 2009. tpsRegr1.37. Stony Brook, NY: Department of Ecology and
762 Evolution, State University of New York.
763 Slater GJ, Van Valkenburgh B. 2008. Long in the tooth: evolution of sabertooth
764 cat cranial shape. Paleobiology 34:403–419.
765 Samuels JX, Van Valkenburgh B. 2008. Skeletal indicators of locomotor
766 adaptations in living and extinct rodents. J Morphol 269:1387–1411.
767 Schutz H, Guralnick RP. 2007. Postcranial element shape and function:
768 assessing locomotor mode in extant and extinct mustelids carnivorans. Zool J
769 Linn Soc 150: 895–914.
770 SPSS Inc. 2009. PASW Statistics 18.0. Chicago: IBM company headquarters.
771 Turner A, Antón M. 1997. The Big Cats and their fossil relatives. New York:
772 Columbia University Press.
773 Van Valkenburgh B. 1987. Skeletal Indicators of Locomotor Behaviour in Living
774 and Extinct Carnivores. J Vertebr Paleont 7:162–182.
775 Werdelin L. 1983. Morphological patterns in the skulls of cats. Biol J Linn Soc
776 19:375–391.
777 Werdelin L, Wesley-Hunt G. 2010. The biogeography of carnivore
778 ecomorphology. In: Goswami A, Friscia A, editors. Carnivoran Evolution: New
779 Views on Phylogeny, Form and Function. New York: Cambridge University
780 Press. p 225–245.
781 Werdelin L, Yamaguchi N, Johnson WE, O'Brien SJ. 2010. Phylogeny and
782 evolution of cats (Felidae). In: MacDonald DW, Loveridge AJ, editors. Biology
783 and Conservation of Wild Felids. Oxford: Oxford University Press. p 59–82.

784 Young, N.M. 2008. A Comparison of the Ontogeny of Shape Variation in the
785 Anthropoid Scapula: Functional and Phylogenetic Signal. American Journal of
786 Physical Anthropology. 136:247–264.
787 Zelditch ML, Swiderski DL, Sheets HD, Fink WL. 2004. Geometric
788 morphometrics for biologists. A primer. Amsterdam: Elsevier.
789
790

791 **FIGURE CAPTIONS**

792 **Fig. 1** The location of landmarks digitised for each epiphyseal aspect.
793 Landmarks are placed to represent anatomical loci of functional significance.
794 Scale bars represent 10 millimetres. Dotted lines demonstrate how angular and
795 linear measurements were used to obtain landmarks geometrically. A = Lateral
796 aspect of the proximal epiphysis, B = Medial aspect of the proximal epiphysis, C
797 = Anterior aspect of the distal epiphysis, D = Posterior aspect of the distal
798 epiphysis. Anatomical position of each landmark as follows: (A1, B1) Most distal
799 point on the humeral head; (A2) proximal junction between humeral head and
800 greater tubercle; (A3*) lies on the anterior surface of the humerus and is
801 perpendicular to the line connecting landmarks A1 & A2, at the level of
802 landmark A2; (A4, B8) proximal tip of the greater tubercle; (A5*) furthest
803 projection of the humeral head, at a distance halfway between landmarks A1 &
804 A2; (B2) most anterior and most distal point on the lesser tubercle; (B3) most
805 anterior and most proximal point on the lesser tubercle; (B4*) lies on the
806 anterior surface of the humerus and is perpendicular to the line connecting
807 landmarks B1 & B3, at the level of landmark B3; (B5) most posterior and most

808 distal point on the lesser tubercle; (B6) most posterior and most proximal point
809 on the lesser tubercle; (B7*) furthest projection of the humeral head at a
810 distance halfway between landmarks B1 & B6; (C1, D2) distal tip of the
811 trochlea; (C2, D3) distal junction between the trochlea and capitulum; (C3, D4)
812 most distal and most lateral point on the capitulum; (C4, D1) most proximal and
813 most lateral point on the capitulum; (C5) proximal tip of the trochlea; (C6)
814 proximal tip of the supracondyloid foramen; (C7, D7) most medial point on the
815 medial epicondyle; (D5) proximal tip of the olecranon fossa; (D6) most lateral
816 point on the lateral epicondyle; (D8*) lies on the medial surface of the olecranon
817 fossa and is perpendicular to the line connecting landmark D1 & D4, at the level
818 of landmark D1. *Landmark obtained geometrically.
819
820 **Fig. 2** Four PC plots describing the scatter of specimens across PC1 and PC2.
821 Each PC plot represents a different epiphyseal aspect; A= Lateral aspect of the
822 proximal epiphysis, B= Medial aspect of the proximal epiphysis, C= Anterior
823 aspect of the distal epiphysis, D= Posterior aspect of the distal epiphysis.
824 Specimens are grouped according to lineage. Transformation grids, at the
825 extremes of each PC, show the relative deformation from the mean shape.
826 Landmarks are linked by a wireframe in all transformation grids.
827
828 **Fig. 3** Transformation grids to demonstrate the relative change in shape from
829 the smallest to the median and to the largest value of NLog centroid size for
830 each epiphyseal aspect. Centroid sizes given in each grid are to 3 significant
831 figures. Letters indicate epiphyseal aspect: A= Lateral aspect of the proximal

832 epiphysis, B= Medial aspect of the proximal epiphysis, C= Anterior aspect of the
833 distal epiphysis, D= Posterior aspect of the distal epiphysis. The smallest NLog
834 centroid size is exhibited by an individual of the species *Prionailurus planiceps*
835 in all cases, excluding the anterior aspect of the distal epiphysis, where the
836 smallest value is provided by a specimen of the species *Felis nigripes*.
837 Specimens of *Caracal caracal* represent the median NLog centroid size in the
838 case of the lateral and medial views of the proximal epiphysis. In the case of the
839 distal epiphysis, specimens are of *Lynx lynx*. Finally, the largest NLog centroid
840 size values are provided by specimens belonging to the species *Panthera leo* in
841 the case of the proximal epiphysis. These values are provided by *Panthera*
842 *tigris* specimens for the distal epiphysis.
843
844 **Fig. 4** Four plots of function 1 vs. function 2 determined by DFAs. The scatter of
845 specimens, categorised according to locomotor group, is shown, with group
846 centroids included. Each plot represents a different epiphyseal aspect; A=
847 Lateral aspect of the proximal epiphysis, B= Medial aspect of the proximal
848 epiphysis, C= Anterior aspect of the distal epiphysis, D= Posterior aspect of the
849 distal epiphysis. Transformation grids, at the extremes of each axis, show the
850 relative deformation from the mean shape. Landmarks are linked by a
851 wireframe in all transformation grids.
852
853 **Fig. 5.** Composite phylogeny of 32 extant species of Felidae showing character
854 mapping based on squared-change parsimony (Maddison and Maddison, 2000)

855 for PC1 species-averaged scores of the four epiphyses analysed. Time of
856 divergence between species are expressed in millions of years.
857 A= Lateral aspect of the proximal epiphysis, B= Medial aspect of the proximal
858 epiphysis, C= Anterior aspect of the distal epiphysis, D= Posterior aspect of the
859 distal epiphysis.

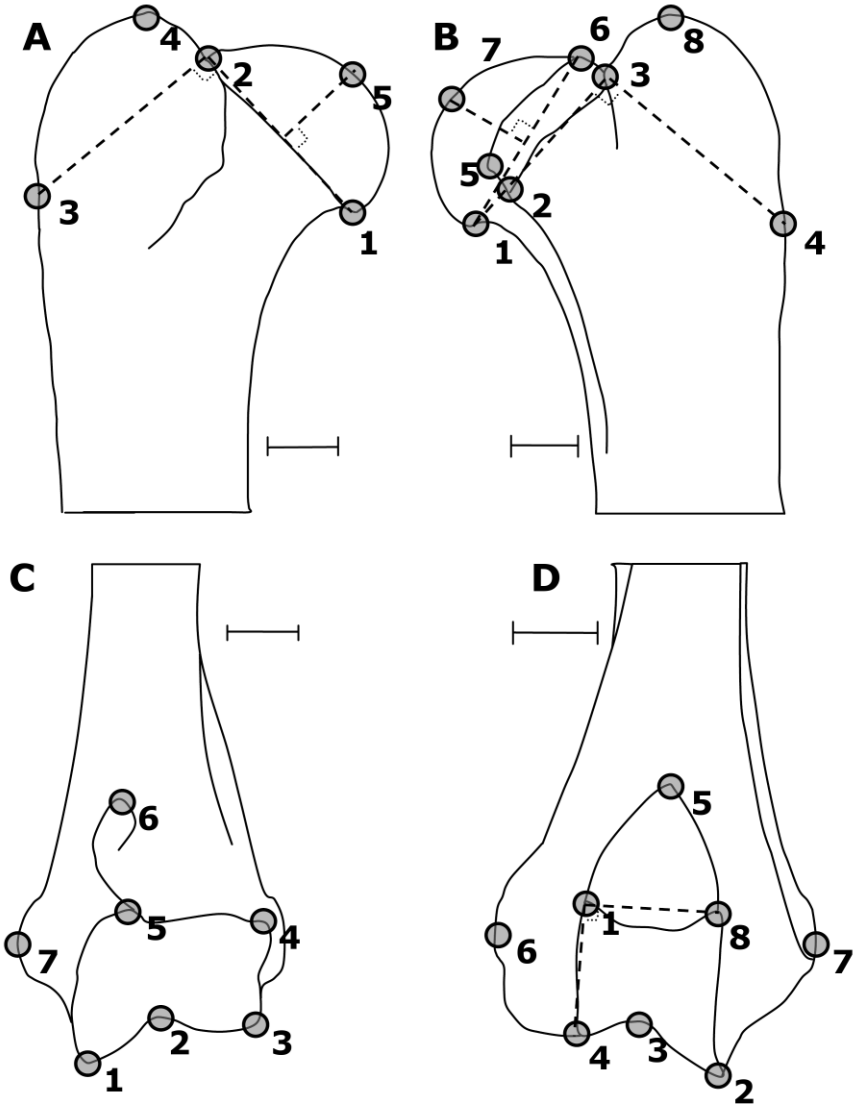
A
4
2
5
3
1
B
7
6
8
3
5
2
1
4
C
6
5
4
7
2
3
1
D
5
1
8
6
7
4
3
2

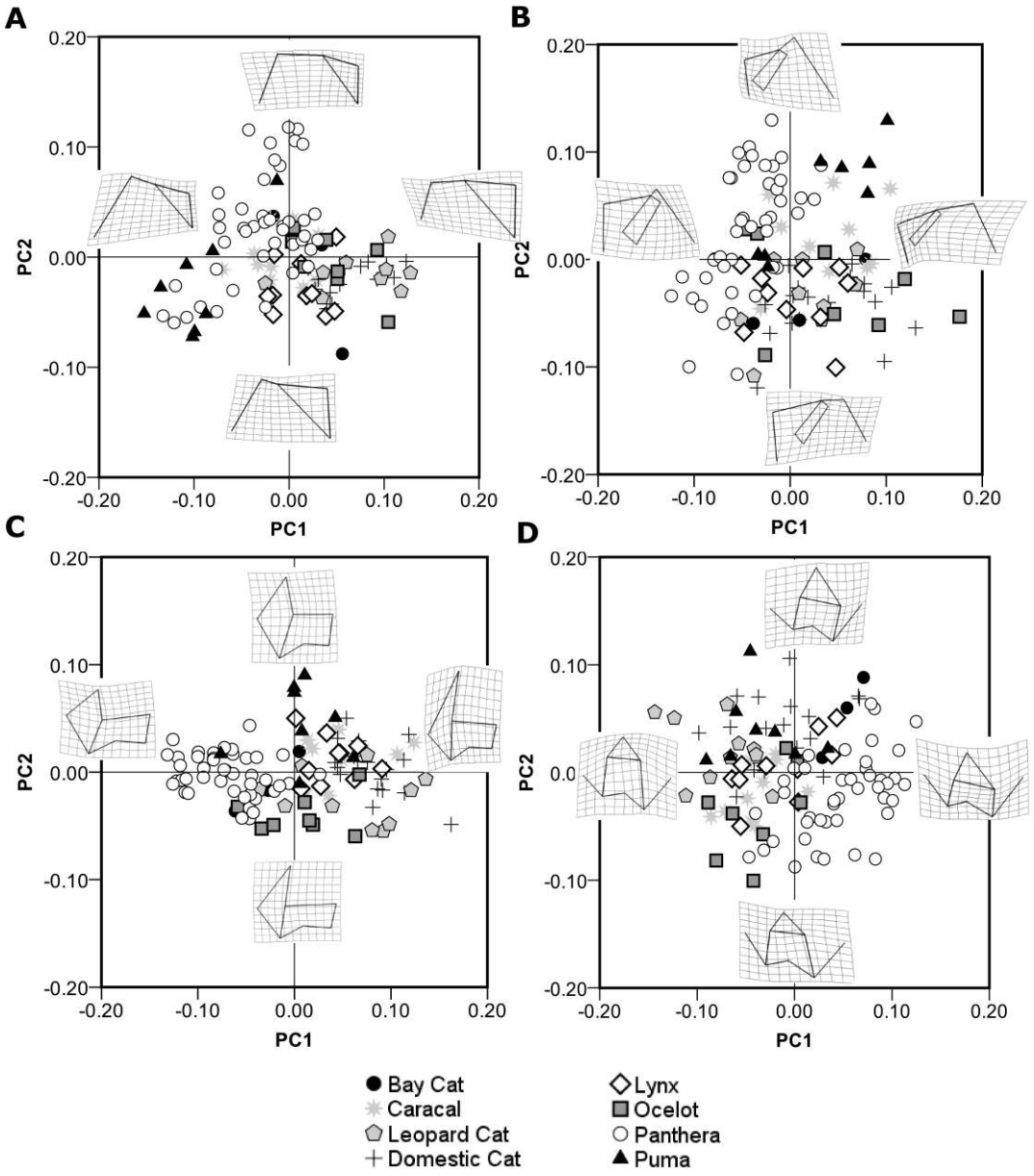
A
B
C
D
PC1
PC2
0.20
0.10
0.00
-0.10
-0.20
Bay Cat
Caracal
Leopard Cat
Domestic Cat
Lynx
Ocelot
Panthera
Puma

A

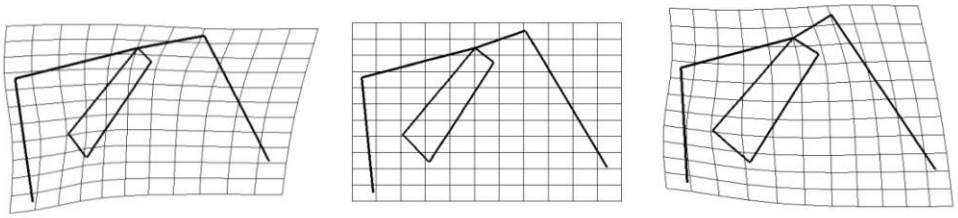

0.322 1.287 2.224

B

0.391 1.374 2.312

C

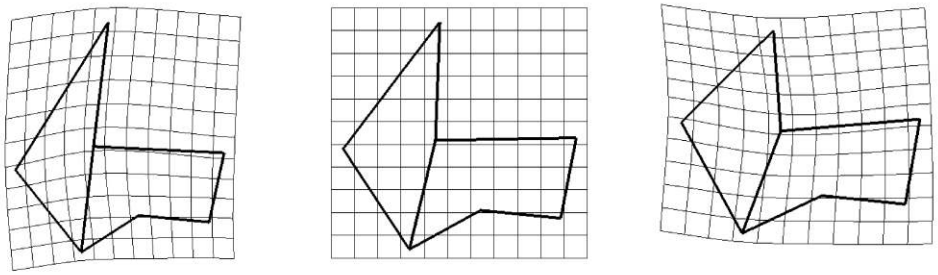

0.439 1.342 2.290

D

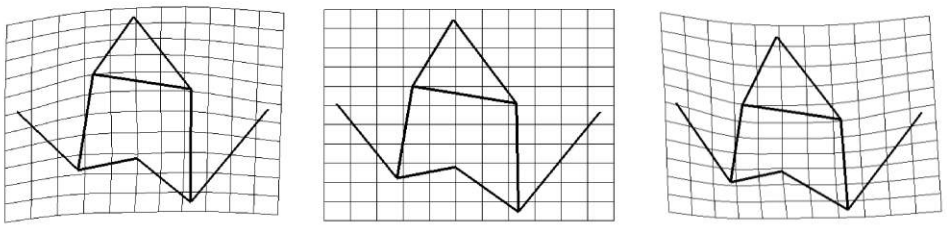

0.321 1.274 2.250

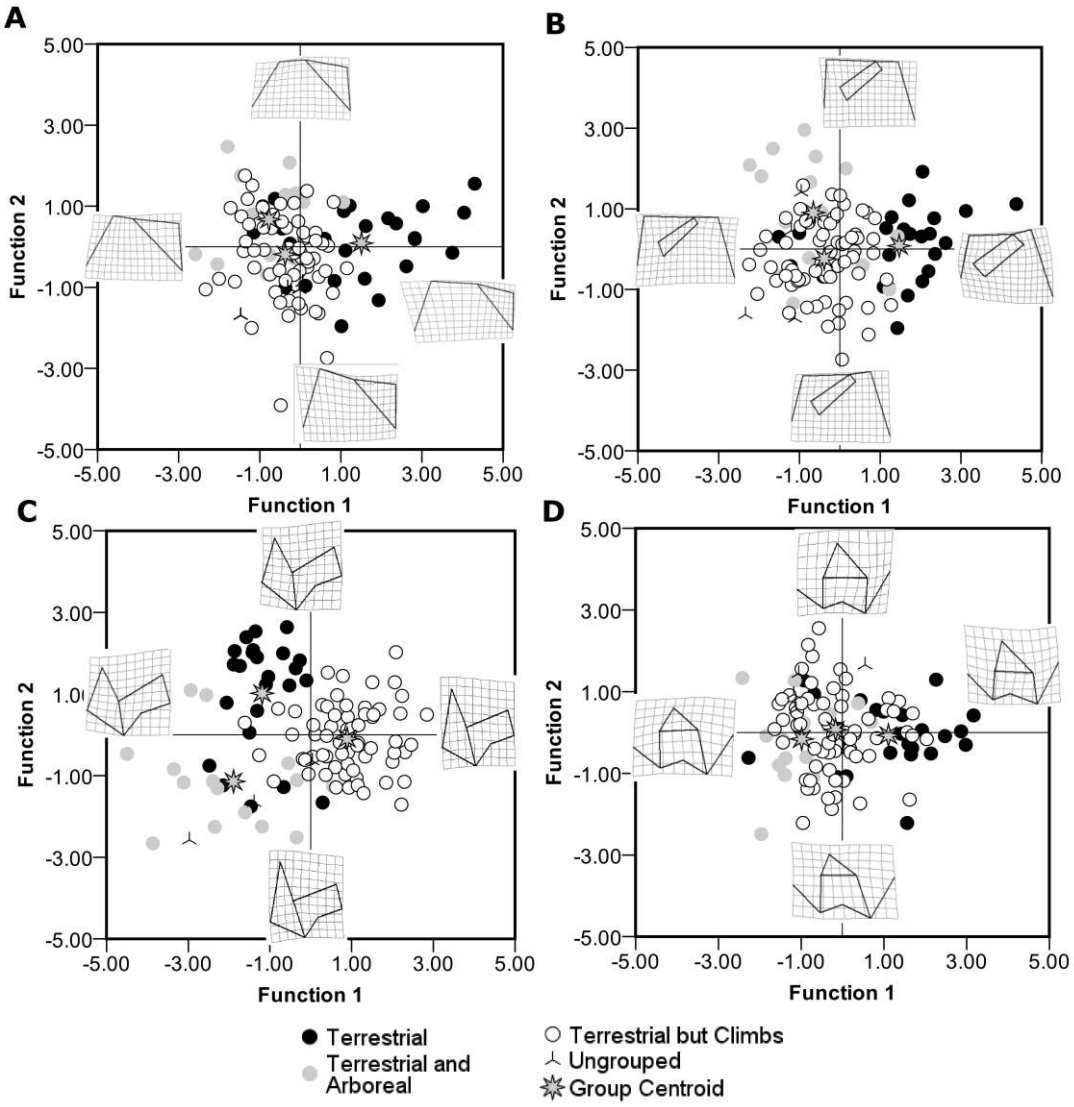
A
B
C
D
Function 1
Function 2
5.00
3.00
1.00
-1.00
-3.00
-5.00
Terrestrial
Terrestrial and Arboreal
Terrestrial but Climbs
Ungrouped
Group Centroid

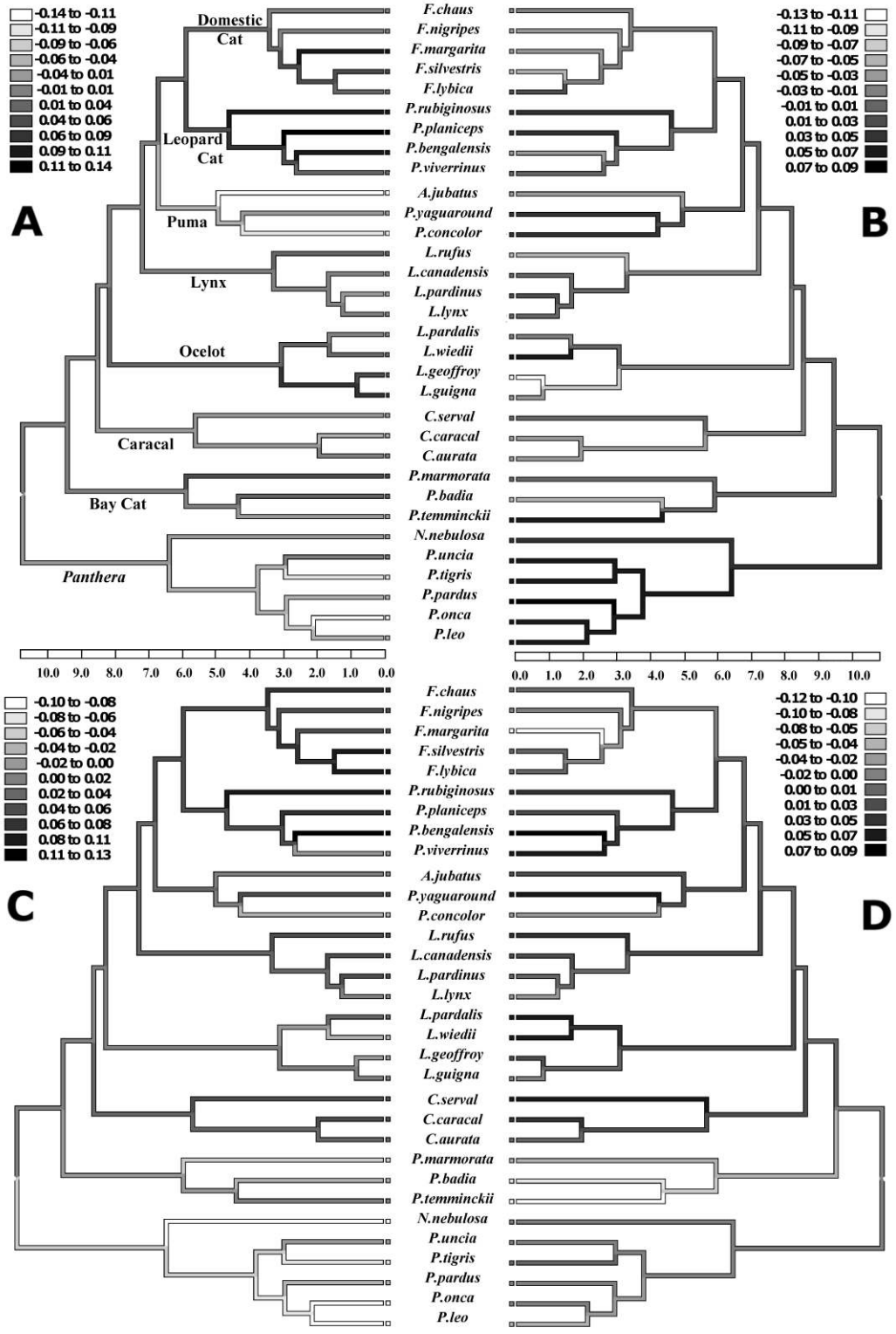
A
B
C
D
-0.14 to -0.11
-0.11 to -0.09
-0.09 to -0.06
-0.06 to -0.04
-0.04 to 0.01
-0.01 to 0.01
0.01 to 0.04
0.04 to 0.06
0.06 to 0.09
0.09 to 0.11
0.11 to 0.14
-0.13 to -0.11
-0.11 to -0.09
-0.09 to -0.07
-0.07 to -0.05
-0.05 to -0.03
-0.03 to -0.01
-0.01 to 0.01
0.01 to 0.03
0.03 to 0.05
0.05 to 0.07
0.07 to 0.09
-0.10 to -0.08
-0.08 to -0.06
-0.06 to -0.04
-0.04 to -0.02
-0.02 to 0.00
0.00 to 0.02
0.02 to 0.04
0.04 to 0.06
0.06 to 0.08
0.08 to 0.11
0.11 to 0.13
-0.12 to -0.10
-0.10 to -0.08
-0.08 to -0.05
-0.05 to -0.04
-0.04 to -0.02
-0.02 to 0.00
0.00 to 0.01
0.01 to 0.03
0.03 to 0.05
0.05 to 0.07
0.07 to 0.09
Domestic Cat
Leopard Cat
Puma
Lynx
Ocelot
Caracal
Bay Cat
Panthera
F.chaus
F.nigripes
F.margarita
F.silvestris
F.lybica
P.rubiginosus
P.planiceps
P.bengalensis
P.viverrinus
A.jubatus
P.yaguaround
P.concolor
L.rufus
L.canadensis
L.pardinus
L.lynx
L.pardalis
L.wiedii
L.geoffroy
L.guigna
C.serval
C.caracal
C.aurata
P.marmorata
P.badia
P.temminckii
N.nebulosa
P.uncia
P.tigris
P.pardus
P.onca
P.leo
10.0 9.0 8.0 7.0 6.0 5.0 4.0 3.0 2.0 1.0 0.0
0.0 1.0 2.0 3.0 4.0 5.0 6.0 7.0 8.0 9.0 10.0

TABLES

Table 1 MANOVA statistic for each epiphyseal aspect, with phylogenetic categories as independent (X) and shape PCs as the dependent (Y) variables. The percentage of variance explained by phylogeny is displayed for each aspect. Significant P values are highlighted in bold.

Epiphysis and aspect	Wilks' Lambda	F	Hypo d.f.	Error d.f.	% variance explained	P value
Lateral aspect, proximal epiphysis	0.140	5.632	42	453.7	45.67	**<0.0001**
Medial aspect, proximal epiphysis	0.032	5.050	84	559.2	33.97	**<0.0001**
Anterior aspect, distal epiphysis	0.045	5.517	70	549.1	53.20	**<0.0001**
Posterior aspect, distal epiphysis	0.028	5.326	84	565.3	35.67	**<0.0001**

Table 2 Statistic for multivariate regression testing allometry with Nlog size as independent (X) variable and shape PCs as dependent (Y). The percentage of variance explained by size is displayed for each epiphyseal aspect. Significant

Epiphysis and aspect	Wilks' Lambda	F	Hypo d.f.	Error d.f.	% variance explained	P value
Lateral aspect, proximal epiphysis	0.272	45.533	6	102	35.35	**<0.0001**
Medial aspect, proximal epiphysis	0.207	30.568	12	96	20.07	**<0.0001**
Anterior aspect, distal epiphysis	0.260	28.150	10	99	40.17	**<0.0001**
Posterior aspect, distal epiphysis	0.205	31.394	12	97	17.01	**<0.0001**

P values are highlighted in bold.

Table 3 MANOVA statistic for each epiphyseal aspect with locomotion categories as independent (X) variables and all shape PCs as the dependent (Y). The percentage of variance explained by locomotion is displayed for each aspect. Significant P values are highlighted in bold. *Pardofelis temminckii*, *Pardofelis badia* and 2 of *Felis nigripes*, were excluded from MANOVA as the locomotor category of these individuals is unknown

Epiphysis and aspect	Wilks' Lambda	F	Hypo d.f.	Error d.f.	% variance explained	P value
Lateral aspect, proximal epiphysis	0.490	6.927	12	194	11.70	**<0.0001**
Medial aspect, proximal epiphysis	0.449	3.731	24	182	4.83	**<0.0001**
Anterior aspect, distal epiphysis	0.360	6.268	20	188	16.09	**<0.0001**
Posterior aspect, distal epiphysis	0.494	3.239	24	184	8.96	**<0.0001**

Table 4 Wilks' Lambda values in addition to degrees of freedom and P values for both functions created in each DFA. Significant P values are highlighted in bold.

Epiphysis and aspect	Function	Wilks' Lambda	d.f.	P value
Lateral aspect, proximal epiphysis	DF1	0.535	6	**<0.0001**
	DF2	0.916	2	**0.012**
Medial aspect, proximal epiphysis	DF1	0.518	10	**<0.0001**
	DF2	0.864	4	**0.006**
Anterior aspect, distal epiphysis	DF1	0.288	12	**<0.0001**
	DF2	0.690	5	**<0.0001**
Posterior aspect, distal epiphysis	DF1	0.682	6	**<0.0001**
	DF2	0.992	2	0.681

Table 5 The composition of each function, showing the variables selected by stepwise procedure and the correlation coefficient (r) loaded on each function. NLog_CS = NLog centroid size, PC = Principal Component of shape variables.

Epiphysis and aspect	Function 1	Function 2
Lateral aspect, proximal epiphysis	PC2 0.793 PC7 0.589 NLog_CS 0.571 PC4 0.284	PC3 0.819 PC6 0.561 PC8 0.798 PC9 0.307
Medial aspect, proximal epiphysis		
Anterior aspect, distal epiphysis	PC9 0.340	NLog_CS 0.731 PC1 -0.444 PC4 -0.439 PC8 0.321 PC3 0.285
Posterior aspect, distal epiphysis	NLog_CS 0.725	PC2 0.756 PC7 -0.650

Table 6 Percentage of correctly classified cases after leave one out procedure, including an overall percentage for each epiphyseal aspect, and specific percentages for each locomotor group.

Epiphysis and aspect	Total %	%Terrestrial	% Terrestrial and Arboreal	% Terrestrial but Climbs
Lateral aspect, proximal epiphysis	62.9	75.0	60.0	59.1
Medial aspect, proximal epiphysis	64.8	83.3	60.0	59.1
Anterior aspect, distal epiphysis	83.0	79.2	62.5	89.4
Posterior aspect, distal epiphysis	50.0	66.7	62.5	40.9

Table 7 Percentage of correctly reclassified specimens for each species in LAPE (lateral aspect of the proximal epiphysis), MAPE (medial aspect of the proximal epiphysis), AADE (anterior aspect of the distal epiphysis) and PADE (posterior aspect of the distal epiphysis). Predicted locomotor categories for the unknown specimens by each DFA are also listed in the table (T but Cl = Terrestrial but Climbs; T and A = Terrestrial and Arboreal). # prox = Number of proximal specimens per species. # dist = Number of distal specimens per species

Species	# prox	# dist	LAPE	MAPE	AADE	PADE
Acinonyx jubatus	5	5	**100.00%**	**100.00%**	80.00%	40.00%
Caracal aurata	2	2	**100.00%**	0.00%	**100.00%**	50.00%
Caracal caracal	2	2	50.00%	50.00%	**100.00%**	**100.00%**
Caracal serval	6	6	50.00%	83.33%	**100.00%**	0.00%
Felis silvestris lybica	3	3	**100.00%**	33.33%	**100.00%**	33.33%
Felis chaus	2	2	**100.00%**	50.00%	**100.00%**	50.00%
Felis margarita	2	2	0.00%	0.00%	0.00%	0.00%
Felis nigripes	2	2	T but Cl	T but Cl	T but Cl	T but Cl
Felis silvestris grampia	9	9	44.44%	66.67%	**100.00%**	22.22%
Leopardus geoffroy	2	2	**100.00%**	50.00%	**100.00%**	50.00%
Leopardus guigna	1	1	0.00%	**100.00%**	**100.00%**	**100.00%**
Leopardus pardalis	4	4	75.00%	25.00%	75.00%	25.00%

Leopardus wiedii	1	1	0.00%	**100.00%**	**100.00%**	**100.00%**
Lynx lynx	3	3	33.33%	**100.00%**	**100.00%**	66.67%
Lynx rufus	1	1	**100.00%**	**100.00%**	**100.00%**	0.00%
Lynx canadensis	4	4	0.00%	0.00%	**100.00%**	50.00%
Lynx pardinus	2	2	**100.00%**	50.00%	50.00%	50.00%
Neofelis nebulosa	3	3	33.33%	33.33%	**100.00%**	**100.00%**
Panthera leo	17	17	**100.00%**	**100.00%**	**100.00%**	94.12%
Panthera onca	3	3	**100.00%**	0.00%	0.00%	0.00%
Panthera pardus	12	12	66.67%	50.00%	83.33%	58.33%
Panthera tigris	4	4	0.00%	50.00%	**100.00%**	25.00%
Panthera uncia	4	4	**100.00%**	**100.00%**	75.00%	50.00%
Pardofelis badia	1	1	T but Cl	T and A	T and A	T and A
Pardofelis marmorata	1	1	**100.00%**	**100.00%**	**100.00%**	**100.00%**
Pardofelis temminckii	1	1	T but Cl	T and A	T but Cl	T and A
Prionailurus bengalensis	3	4	33.33%	**100.00%**	33.33%	66.67%
Prionailurus planiceps	1	1	0.00%	0.00%	0.00%	0.00%
Prionailurus rubiginosus	1	1	**100.00%**	**100.00%**	**100.00%**	**100.00%**
Prionailurus viverrinus	4	4	25.00%	75.00%	50.00%	0.00%
Puma concolor	2	2	0.00%	50.00%	50.00%	**100.00%**
Puma jagouaroundi	1	1	0.00%	**100.00%**	**100.00%**	0.00%

Table 8 Percentage of correctly classified cases after leave one out procedure with specimens of *Panthera leo, Felis silvestris* or *Neofelis nebulosa* individually excluded, including an overall percentage for each epiphyseal aspect, and specific percentages for each locomotor group. # Sample prox/dist = Number of specimens used in proximal epiphyseal analyses / Number of specimens used in distal epiphyseal analyses

	Epiphysis and aspect	Total %	%Terrestrial	% Terrestrial and Arboreal	% Terrestrial but Climbs
Excluding *P.leo*. # Sample prox/dist = 88/89	Lateral aspect, proximal epiphysis	54.5	71.4	53.3	53.0
	Medial aspect, proximal epiphysis	56.8	71.4	46.7	57.6
	Anterior aspect, distal epiphysis	83.1	85.7	56.3	89.4
	Posterior aspect, distal epiphysis	59.6	57.1	31.3	66.7
Excluding *F.silvestris* # Sample prox/dist = 96/97	Lateral aspect, proximal epiphysis	69.8	75.0	60.0	70.2
	Medial aspect, proximal epiphysis	62.5	70.8	60.0	59.6
	Anterior aspect, distal epiphysis	81.4	79.2	62.5	87.7
	Posterior aspect, distal epiphysis	58.8	66.7	56.3	56.1
Excluding *N.nebulosa* # Sample prox/dist = 102/103	Lateral aspect, proximal epiphysis	67.6	75.0	58.3	66.7
	Medial aspect, proximal epiphysis	69.6	75.0	66.7	68.2
	Anterior aspect, distal epiphysis	81.6	79.2	61.5	86.4
	Posterior aspect, distal epiphysis	64.1	66.7	61.5	63.6

Table 9 Phylogenetic Generalised Least Squares models for locomotor categories or allometry, showing Wilks' Lambda, F test, degrees of freedom and probability values. Significant P values are highlighted in bold.

	Epiphysis and aspect	**Wilks' Lambda**	**F**	**d.f. 1**	**d.f. 2**	**P value**
PGLS Locomotion	Lateral aspect, proximal epiphysis	0.385	2.448	12.0	48.0	**0.0141**
	Medial aspect, proximal epiphysis	0.371	0.961	24.0	36.0	0.5317
	Anterior aspect, distal epiphysis	0.228	2.186	20.0	40.0	**0.0174**
	Posterior aspect, distal epiphysis	0.199	1.864	24.0	36.0	**0.0442**
PGLS Size	Lateral aspect, proximal epiphysis	0.403	6.169	6.0	25.0	**0.0005**
	Medial aspect, proximal epiphysis	0.234	5.179	12.0	19.0	**0.0008**
	Anterior aspect, distal epiphysis	0.494	2.147	10.0	21.0	0.0674
	Posterior aspect, distal epiphysis	0.191	6.708	12.0	19.0	**0.0001**